Rotational Alignment of Products from the NOCl + Ca Chemiluminescent Reaction

Ji-Ping Zhan, He-Ping Yang, Ke-Li Han,* Wei-Qiao Deng, Guo-Zhong He, and Nan-Quan Lou

State Key Laboratory of Molecular Reaction Dynamics, Dalian Institute of Chemical Physics, Chinese Academy of Sciences, Dalian 116023, People's Republic of China

Received: February 11, 1997; In Final Form: April 18, 1997[⊗]

The product rotational alignment $\langle P_2(\hat{\mathbf{J}}'\cdot\hat{\mathbf{k}})\rangle = -0.35 \pm 0.04, -0.15 \pm 0.02$ for CaCl(B), CaCl(A) are obtained from Ca + NOCl chemiluminescent reactions, respectively. The experiments are carried out under single collision conditions in a beam−gas apparatus. Quasi-classical trajectory (QCT) calculations for Ca + NOCl reaction have been carried out. The calculated results agree well with the experimental ones. The strong product alignments for the reactions are attributed to attractive potential surfaces. It is plausible that the difference of the rotational alignment between the $A^2\Pi$ and $B^2\Sigma$ states of the products is due to their different potential energy surfaces (PESs).

1. Introduction

Theoretical and experimental interest in vector correlation in the reaction processes

$$A + BC \rightarrow AB + C \tag{1}$$

has increased significantly in recent decades.[1] Only by understanding the scalar and vector properties together, as well as possible correlations among them, can the fullest pictures of the scattering dynamics emerge. In order to investigate the vector correlation in the scattering process, not only the magnitudes but also well-defined directions of the vectors during the scattering process should be determined experimentally or theoretically. Energy conservation can give information on the translational and rotational energies that can be directly related to the magnitudes of the velocity and the angular momentum, while angular momentum conservation can give information on both the magnitudes and directions of the vectors.

With the development of the laser and other experimental techniques, the study of correlation of vectors in a reaction became possible. Several experimental methods, such as polarization-resolved chemiluminescence, polarized laser-induced fluorescence, electric deflection methods, REMPI, etc., have been developed to study orientation and alignment in chemical reaction under molecular-beam and bulb conditions.[2−26] Among them, the method of chemiluminescence combined with molecular beams is the simplest and easiest, although this type of method is limited to the reactions giving products chemiluminescence.

From the theoretical side, Hijazi and Polanyi used QCT methods on two potential energy surfaces, one attractive and one repulsive, to investigate the effects of different mass combinations of reactants on the distribution of angles between product rotational angular momentum and reactant relative velocity and the role of reactant orbital angular momentum in determining $\mathbf{J}'$.[27,28] Recently, Han et al. reported the product rotational alignment of several mass combination reactions as a function of collision energies on attractive and repulsive potential surfaces.[29] In another paper of Han et al.,[33] the impulse model indicated that either low repulsive energies, large orbital angular momentum of reactants, or H′ + HL mass combination may lead to strong alignment of the product rotation.

2. Theory

A. Rotational Alignment. During a reactive encounter, the total angular momentum is conserved

$$\mathbf{J} + \mathbf{L} = \mathbf{J}' + \mathbf{L}' \tag{2}$$

where $\mathbf{L}$ and $\mathbf{L}'$ are the orbital momenta of reactant and product, respectively. When the reactant angular momentum $\mathbf{J}$ is small (as is common), the product rotational angular momentum can only result from $\mathbf{L}$. The distribution of the angular momentum $\mathbf{J}'$ of the product molecule is described by a function $f(\hat{\mathbf{J}}'\cdot\hat{\mathbf{Z}})$. The usually experimental configurations possess cylindrical symmetry in space, while a cylindrical symmetrical distribution of the rotational angular momentum of the products can be expressed as a Legendre expansion

$$f(\hat{\mathbf{J}}'\cdot\hat{\mathbf{Z}}) = \sum_1 a_1 P_1(\hat{\mathbf{J}}'\cdot\hat{\mathbf{Z}}) \tag{3}$$

in which $\mathbf{Z}$ denotes the symmetry axis, and carats denote unit vectors. The coefficients a_1 and a_2, which are proportional to $\langle P_1(\hat{\mathbf{J}}'\cdot\hat{\mathbf{Z}})\rangle$ and $\langle P_2(\hat{\mathbf{J}}'\cdot\hat{\mathbf{Z}})\rangle$, are used to describe the orientation and alignment of the products, respectively (the angular brackets appearing above and later denote the average of the items). In a chemiluminescent reaction experiment, the degree of polarization of chemiluminescence P can be related to the distribution of the angular momentum vectors of the emitting molecule

$$P(\text{P,R line}) = -3\langle P_2(\hat{\mathbf{J}}'\cdot\hat{\mathbf{Z}})\rangle/(4 - \langle P_2(\hat{\mathbf{J}}'\cdot\hat{\mathbf{Z}})\rangle) \tag{4}$$

$$P(\text{Q line}) = 3\langle P_2(\hat{\mathbf{J}}'\cdot\hat{\mathbf{Z}})\rangle/(2 + \langle P_2(\hat{\mathbf{J}}'\cdot\hat{\mathbf{Z}})\rangle) \tag{5}$$

where

$$P = (I_{\parallel} - I_{\perp})/(I_{\parallel} + I_{\perp}) \tag{6}$$

The rotational alignment in the laboratory frame should be converted into the center of mass frame by using the expression

$$\langle P_2(\hat{\mathbf{J}}'\cdot\hat{\mathbf{k}})\rangle = \langle P_2(\hat{\mathbf{J}}'\cdot\hat{\mathbf{Z}})\rangle/\langle P_2(\hat{\mathbf{k}}'\cdot\hat{\mathbf{Z}})\rangle \tag{7}$$

for a beam−gas reaction, $\langle P_2(\hat{\mathbf{k}}'\cdot\hat{\mathbf{Z}})\rangle$is given by Monte Carlo calculation.[26]

The expected values for $\langle P_2(\hat{\mathbf{J}}'\cdot\hat{\mathbf{k}})\rangle$ are between 0.0 (randomly aligned) and −0.5 (completely aligned), and when the conditions $|\mathbf{L}| >> |\mathbf{J}|$ and $|\mathbf{L}'| << |\mathbf{J}'|$ are satisfied, the maximum product

* Author to whom correspondence should be addressed.

[⊗] Abstract published in *Advance ACS Abstracts,* September 15, 1997.

S1089-5639(97)00535-5 CCC: $14.00

rotational alignment occurs. The first condition is satisfied if a reaction has large cross-sections, while the typical H + HL mass configuration reaction system leads to the second condition. Several example reactions are as follows: Cs + HI, HBr-($\langle P_2(\hat{\mathbf{J}}'\cdot\hat{\mathbf{k}})\rangle = -0.44, -0.38$), K + HBr($\langle P_2(\hat{\mathbf{J}}'\cdot\hat{\mathbf{k}})\rangle = -0.42$)[11] and Ca(^{1}D) + HCl($\langle P_2(\hat{\mathbf{J}}'\cdot\hat{\mathbf{k}})\rangle = -0.44$).[26]

Recently, Spence and Levy[38] have developed a method for estimating $\langle P_2(\hat{\mathbf{J}}'\cdot\hat{\mathbf{Z}})\rangle$ from chemiluminescent spectra with unresolved rotational branches for a high-J limit. They gave the following expression:

$$R_{\text{obs}} = \frac{\langle P_2(\hat{\mathbf{J}}'\cdot\hat{\mathbf{Z}})\rangle(6\alpha - \langle P_2(\hat{\mathbf{J}}'\cdot\hat{\mathbf{Z}})\rangle - 2)}{(4 - 3\langle P_2(\hat{\mathbf{J}}'\cdot\hat{\mathbf{Z}})\rangle\alpha + 2\langle P_2(\hat{\mathbf{J}}'\cdot\hat{\mathbf{Z}})\rangle)} \quad (8)$$

where α is the fraction of the intensity in the Q branch. In Hund's case b, $\alpha = 0.5$. In pure Hund's case a, $\alpha = 1$. In parallel band, $\alpha = 0$. R_{obs} is the alignment index

$$R_{\text{obs}} = (I_{||} - I_{\perp})/(I_{||} + 2I_{\perp}) \quad (9)$$

B. Potential Energy Surface. The extended LEPS potential energy surface (PES) of a triatomic system is employed in the QCT calculations[30]

$$V(r_1, r_2, r_3) = Q_1 + Q_2 + Q_3 - (J_1^2 + J_2^2 + J_3^2 - J_1J_2 - J_2J_3 - J_3J_1)^{1/2} \quad (10)$$

where

$$Q_i = ({}^1E_i + {}^3E_i)/2 \quad (11)$$

$$J_i = ({}^1E_i - {}^3E_i)/2 \quad (12)$$

${}^1E_i$ and ${}^3E_i$ stand for the Morse potential and anti-Morse potential functions of the diatomic molecule, respectively,

$${}^1E_i = D_i(\{1 - \exp[-\beta_i(r_i - r_i^0)]\}2 - 1) \quad (13)$$

$${}^3E_i = {}^3D_i(\{1 + \exp[-\beta_i(r_i - r_i^0)]\}2 - 1) \quad (14)$$

where

$${}^3D_i = D_i(1 - S_i)/2(1 + S_i) \quad (15)$$

S_i is the adjustable Sato parameter. Subscript $i = 1, 2, 3$ indicates AB, BC, and CA, respectively.

3. Experimental Section

The experiment is carried out in a beam−gas apparatus, which was described in detail elsewhere.[30] Ca metal is heated to 1030 K in an oven. The beam of metal atoms effuses from the oven and then enters the reaction chamber through a 0.3×1 cm^2 rectangular hole. The reaction chamber has been filled with reaction gas. The pressure of the reaction gas is lower than 0.02 Pa, in order to satisfy single collision conditions.

The chemiluminescence of the nascent product CaCl(A) and CaCl(B) is collected by a 15 cm focal length lens positioned at right angles to the metal beam. A film polarizer is placed in front of a 1 m monochromator. A photomultiplier (PMT; RCA C31034) is placed behind the monochromator to detect both perpendicular and parallel components of the chemiluminescence. The output of the PMT is collected by a lock-in amplifier. The response of the optical system, including the monochromator, to the polarized light has been carefully calibrated.

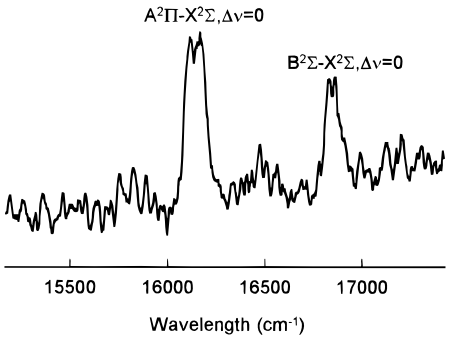

Figure 1. Chemiluminescent spectrum of reaction Ca + NOCl.

The chemiluminescence for the reaction is detected in the range of 15 500−17 350 cm^{-1}. The spectrum is attributed to CaCl, $\Delta\nu = 0$, 1 vibrational bands of $A^2\Pi - X^2\Sigma^+$ and $\Delta\nu = 0$ vibrational bands of $B^2\Sigma + - X^2\Sigma^+$.

4. Results and Discussions

Figure 1 shows the product CaCl* chemiluminescent spectrum for the Ca + NOCl → CaCl* + NO reactions. Both of the transitions $A^2\Pi - X^2\Sigma^+$ and $B^2\Sigma^+ - X^2\Sigma^+$ are observed. The branching ratio for A and B excited states is 2.57:1 Obenauf et al.[32] obtained the branching ratio for the ground state and A, B excited states of this reaction in a low-pressure diffusion flame experiment, and their result is 1538:2.85:1. The branching ratio of A to B states is close to the result obtained by us. According to statistical theory, the corresponding statistical or "prior" branching ratios are given by

$$P_\alpha = g_\alpha\rho_\alpha(E_\alpha)/\sum_\alpha g_\alpha\rho_\alpha(E_\alpha) \quad (16)$$

where α denotes individual states of the product, g_α is the statistical weight factor of each electronic state, $\rho_\alpha(E_\alpha)$ is the quantum phase space density of the corresponding states, and E_α is the available energy for the α excited state. Taking the NO molecule as a harmonic oscillator, we obtained the theoretical prediction of the branching ratio for the product CaCl in X, A, and B states as 2000:8:1. Comparing the theoretical prediction with the experimental observation, we found that the experimental results and the theoretical one of the branching ratio of $B^2\Sigma$ to $X^2\Sigma$ states coincide well, but the branching ratios of the $A^2\Pi$ to $X^2\Sigma$ states do not coincide with each other. Because both the X and B states are Σ^+ states, the reactions for these two products probably possess similar potential surfaces. However, as the A state is a Π state, the potential surface for producing the $A^2\Pi$ state may be different from the other two.

The degree of polarization of the CaCl($A^2\Pi$,$B^2\Sigma^+ - X^2\Sigma^+$) transition is obtained by detecting the parallel and perpendicular polarized components of the chemiluminescence referring to the direction of the beam. For $\Sigma - \Sigma$ transition, only P and R branches can be observed and expressions 4 and 7 and the Monte Carlo calculation results,[26] give the rotational alignment parameter in the center of mass frame as $\langle P_2(\hat{\mathbf{J}}'\cdot\hat{\mathbf{k}})\rangle = -0.35 \pm 0.04$. For $A^2\Pi$ to $X^2\Sigma$ transition, either a P or an R branch and a Q branch are present. Using expression 9, with $\alpha = 1$, i.e. Hund's case a, we obtained $\langle P_2(\hat{\mathbf{J}}'\cdot\hat{\mathbf{k}})\rangle = -0.15 \pm 0.02$. A summary of the results is listed in Table 1.

The $\langle P_2(\hat{\mathbf{J}}'\cdot\hat{\mathbf{k}})\rangle$ of product CaCl(B) for Ca + ClNO reaction system approaches the limit −0.5. As mentioned above, typically, the rotational angular momentum of the product for a large cross-section H′ + HL → H′H + L reaction will be strongly aligned, but the mass combination of the Ca + ClNO

TABLE 1: Summary of Product Alignment for the Experiments

emitter	P_{CL}[a]	R_{CL}[b]	$\langle P_2(\hat{\mathbf{J}}'\cdot\hat{\mathbf{Z}})\rangle$	$\langle P_2(\hat{\mathbf{J}}'\cdot\hat{\mathbf{k}})\rangle$
CaCl(B)	0.195 ± 0.02	0.14 ± 0.02	-0.278 ± 0.03	-0.35 ± 0.04
CaCl(A)	-0.192 ± 0.03	-0.12 ± 0.02	-0.12 ± 0.02	-0.15 ± 0.02

[a] Defined by expression 6. [b] Defined by expression 9.

TABLE 2: LEPS Parameters of the Reaction Ca + NOCl → CaCl + NO for QCT Calculation

species	D_e (kcal/mol)	β (10^8 cm^{-1})	r^0 (10^{-8} cm)	Sato param
	I. Ca + NOCl → CaCl($B^2\Sigma^+$) + NO			
CaCl(B)[a]	46.7	1.517	2.439	0.21
(NO)Cl[b]	34.5	1.485	1.975	0.01
Ca(NO)[c]	10.6	3.996	2.271	−0.9
	II. Ca + NOCl → CaCl($A^2\Pi$) + NO			
CaCl(A)[a]	48.7	1.520	2.439	0.01
(NO)Cl[b]	34.5	1.485	1.975	0.67
Ca(NO)[c]	10.6	3.996	2.271	−0.93

[a] From ref 34. [b] D_e comes from ref 37, ω_e, and r^0 come from ref 35. [c] D_e and r^0 are *ab-initio* calculation results; ω_e comes from ref 36.

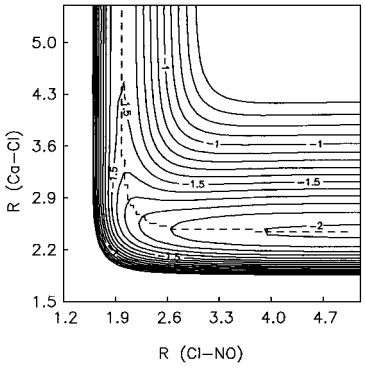

Figure 2. Potential contour map representing the model LEPS for the collinear configuration of reaction Ca + NOCl → CaCl(B) + NO. The contour energies are in electronvolts, and distances are in angstroms. The dashed curve represents the minimum energy path.

reaction is far from the H′ + HL mass combination. Why is the product CaCl(B) rotation strongly aligned for the reaction?

We attribute the strong rotational alignment to the attractive potential. According to theoretical predictions of Han et al.,[29] for an attractive potential surface, the rotational alignment increases with collisional energies for a light light−light (or heavy heavy−heavy) mass combination. At high collisional energies, the orbital angular momentum of the reactants is large, while the rotational excitation comes from both the orbital angular momentum of the reactants and the repulsion between the products. The contribution of the repulsion between the products to the direction of the rotational angular momentum of the products may differ from that of the orbital momentum of the reactants. The repulsive energy gives a distribution of rotational angular momentum vectors of the products which is less anisotropic. Clearly, the higher the collisional energies are, the stronger the rotational alignment of the products will be. In a strong attractive surface for Ca + NOCl reaction, the product rotation may be strongly aligned even at very low collisional energies.

An extended LEPS surface potential surface is obtained for the Ca + NOCl → CaCl(B) + NO using parameters listed in Table 2. A contour plot of this LEPS potential surface is given in Figure 2. The minimum energy reaction path is shown by a dashed line, along which the potential energy decreases monotonically from the entrance ($R_{Ca,NOCl} = \infty$, corresponding to reactants) to the exit ($R_{NO,CaCl} = \infty$, corresponding to products). A set of 100 000 trajectories was sampled for

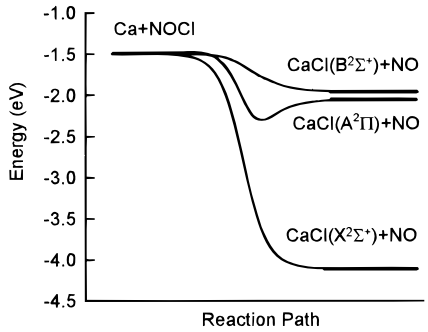

Figure 3. Potential energy profiles along the reaction path of the collinear Ca + NOCl system. The schematic drawing is plotted according to the LEPS potential energy surfaces that were used in QCT calculations. The Sato parameters for X and B states of CaCl are the same (see Table 2), i.e. 0.21, 0.01, and −0.9 for S_{AB}, S_{BC}, and S_{CA}, respectively. While the Sato parameters for the A state of CaCl are 0.01, 0.67, and −0.93.

collision energy at 2.0 kcal/mol. The QCT calculated result of $\langle P_2(\hat{\mathbf{J}}'\cdot\hat{\mathbf{k}})\rangle = -0.35$ was obtained, which agreed very well with the experimental one.

It is apparent that the rotational alignment of the $A^2\Pi$ state of CaCl is much weaker than that of the $B^2\Sigma$ state. The reason may be that the PES for producing the two states of products are different. In fact, our QCT calculation shows that the PES for the two channels of the Ca + NOCl reaction are quite different. The potential surface for producing CaCl($B^2\Sigma$) does not have a barrier or well and slopes down from the entrance of the surface to the exit of the surface, while the PES for yielding product in the $A^2\Pi$ state has a well (See Figure 3). This well will have an apparent influence on the rotational alignment of the product. The molecule may move directly from the entrance of the PES to the exit of the PES for producing the $B^2\Sigma$ state of CaCl, while on the PES for producing the $A^2\Pi$ state of CaCl the movement of the molecule may be trapped in the potential well for a long time, before exiting to the product channel. In the latter case, the reaction intermediate may partly lose its memory of angular momentum; at the same time, the separation of the products will take various directions in space, and the orbital angular momentum of the products will also take various directions. This leads to a weakening of the rotational alignment of the products.

Figure 4 shows the dependence of $\langle P_2(\hat{\mathbf{J}}'\cdot\hat{\mathbf{k}})\rangle$ on the impact parameter at the collisional energy of 2 kcal/mol. The rotational alignment is weak at moderate impact parameters but is strong at both large and small impact parameters. This is explained as follows: at large impact parameters, on the one hand, the orbital angular momentum of the reactants is large in magnitude, and this directly results in the strong rotational alignment of the product; on the other hand, the scattering directions of the products are almost the same as the relative velocity directions of the reactants that is, the orbital angular momenta of the reactants and products are almost parallel. Therefore, the rotational angular momenta of the products are strongly aligned. However, at small impact parameter, the products are scattered backward, the orbital angular momentum of the products may be parallel, but opposed, to the rotation angular momentum of the products; this will lead to strong alignment of the product rotation as well. While at the moderate impact parameter, the directions of the orbital angular momentum of the products are most probably different from that of the orbital angular momentum of the reactants; this results in weak alignment of the product rotation. The weakest alignment corresponds to scattering angles of 90−100°.

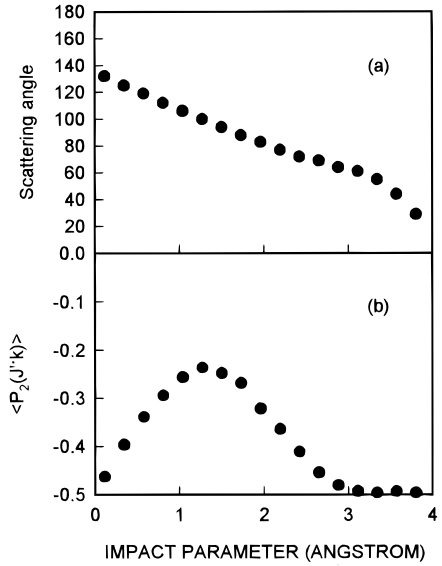

Figure 4. (a) Dependence of the product rotational alignment on the impact parameter. (b) Dependence of the average scattering angle on the impact parameter. Both are at a collisional energy of 2 kcal/mol.

5. Conclusions

Experimental investigations of product rotational alignments for the beam−gas chemiluminescence reaction Ca + NOCl → CaCl(A,B) + NO were carried out. The rotational alignments for product CaCl(B) is strong, even though the mass combination for these reaction systems are far away from the typical H′ + HL → H′H + L reaction. The strongly rotational alignment is attributed to the attractive PES of the reactions.

The branching ratio of products CaCl(B):CaCl(A) = 1:2.57 was experimentally determined and deviates from a statistical prediction. This may be caused by the different features of the potential surfaces for producing the two different states. The different characters between the potential surfaces also causes the difference of the rotational alignment between the $A^2\Pi$ and $B^2\Sigma$ states of the products.

The QCT calculation on the extended LEPS surface for producing CaCl(B) was carried out. The calculation result coincides well with the experimental one. In addition, the calculated results show the dependence of the product rotation alignment on the impact parameter. The strong alignment corresponds to both small and large impact parameters, while the weak alignment corresponds to a moderate impact parameter.

Acknowledgment. This work is supported in part by the National Science Foundation of China and the State Committee of Science and Technology of China.

References and Notes

(1) Orr-Ewing, A. J.; Zare, R. N. *Annu. Rev. Phys. Chem.* **1994**, *45*, 315.

(2) Jonah, C. D.; Zare, R. N.; Ottinger, Ch. *J. Chem. Phys.* **1972**, *56*, 263.

(3) Rettner, C. T.; Simons, J. P. *Chem. Phys. Lett.* **1978**, *59*, 178.

(4) Rettner, C. T.; Simons, J. P. *Faraday Discuss. Chem. Soc.* **1979**, *67*, 329.

(5) Hennessy, R. J.; Simons, J. P. *Chem. Phys. Lett.* **1980**, *75*, 43.

(6) Prisant, M. G.; Rettner, C. T.; Zare, R. N. *Chem. Phys. Lett.* **1982**, *88*, 271.

(7) Engelke, F.; Meiwes-broer, K. H. *Chem. Phys. Lett.* **1984**, *108*,-132.

(8) Jalink, H.; Parker, D. H.; Stolte, S. *J. Chem. Phys.* **1986**, *85*, 5372.

(9) Ondrey, G.; Veen, N. Van; Bersohn, R. *J. Chem. Phys*. **1983**, *78*, 3732.

(10) Hall, G. E.; Sivakumar, N.; Houston, P. L.; Burak, I. *Phys. Rev. Lett.* **1986**, *56*,1671.

(11) Hsu, D. S. Y.; Weinstein, N. D.; Herschbach, D. R. *Mol. Phys.* **1975**, *29*, 257.

(12) Maltz, C.; Weinstein, N. D.; Herschbach, D. R. *Mol. Phys.* **1972**, *24*, 133.

(13) Hsu, D. S. Y.; McClelland, G. M.; Herschbach, D. R. *J. Chem. Phys*. **1974**, *61*, 4927.

(14) Vries, M. S. de; Tyndall, G. W.; Cobb, C. L.; Martin, R. M. *J. Chem. Phys*. **1986**, *84*, 3753.

(15) Hsu, D. S. Y.; Herschbach, D. R. *Faraday Discuss. Chem. Soc*. **1973**, *55*, 116.

(16) Tyndall, G. W.; Vries, M. S. de; Cobb, C. L.; Martin, R. M. *Chem. Phys. Lett*. **1992**, *195*, 279.

(17) Li, R. J.; Han, K. L.; Li, F. E.; Lu, R. C.; He, G. Z.; Lou, N. Q. *Chem. Phys. Lett*. **1994**, *220*, 281.

(18) Li, R. J.; Li, F. E.; Han, K. L.; Lu, R. C.; He, G. Z.; Lou, N. Q. *Proc. Int. Conf. Laser '92* **1993**; 456.

(19) Hennessy R. J.; Simons. J. P. *Mol. Phys*. **1982**, *43*, 181.

(20) Menedez, M.; Garay, M.; Verdasco, E.; Castano, J.; Gonzalez-Urena, A. *J. Phys. Chem*. **1993**, *97*, 5836.

(21) Green, F.; Hancock, G.; Orr-Ewing, A. J. *Faraday Discuss. Chem. Soc*. **1991**, *91*, 79.

(22) Costen, M. L.; Hancock, G.; Orr-Ewing, A. J.; Summerfield, D. *J. Chem. Phys*. **1994**, *100*, 2754.

(23) Sauder, D. G.; Stephenson, J. C.; King, D. S.; Casassa, M. P. *J. Chem. Phys*. **1992**, *97*, 952.

(24) Kleinermanns, K.; Linnebach, E. *Appl. Phys. B* **1986**, *36*, 203.

(25) Zande, W. Van der; Zhang, R.; McKendrick, K. G.; Zare, R. N.; Valentini, J. J. *J. Phys. Chem*. **1991**, *95*, 8205.

(26) Prisant, M. G.; Rettner, C. T.; Zare, R. N. *J. Chem. Phys*. **1981**, *75*, 2222.

(27) Hijazi, N. H.; Polanyi, J. C. *Chem. Phys*. **1975**, *11*, 1.

(28) Hijazi, N. H.; Polanyi, J. C. *J. Chem. Phys*. **1975**, *63*, 2249.

(29) Han, K. L.; He, G. Z.; Lou, N. Q. *J. Chem. Phys*. **1996**, *105*, 8694.

(30) Han, K. L.; Zheng, X. G.; Sun, B. F.; He, G. Z. *Chem. Phys. Lett*. **1991**, *181*, 474.

(31) He, G. Z.; Wang, J.; Tse, R. S.; Lou, N. Q. *Can. J. Chem*. **1988**, *66*, 1936.

(32) Obenauf, R. H.; Hsu, C. J.; Palmer, H. B. *J. Chem. Phys*. **1973**, *58*, 4693.

(33) Li, R. J.; Han, K. L.; Li, F. E.; Lu, R. C.; He, G. Z.; Lou, N. Q. *Chin. J. Chem. Phys*. **1993**, *6*, 1.

(34) Huber, K. P.; Herzberg, G. *Molecular Spectra and Molecular Structure VI*; Van Nostrand: New York, 1979.

(35) McDonald, J. K.; Merritt, J. A.; Kalasinsky, V. F.; Heusel, H. L.; Durig, J. R. *J. Mol. Spectrosc.* **1986**, *117*, 69.

(36) Tevault, D. E.; Andrews, L. *Chem. Phys. Lett*. **1977**, *48*, 103.

(37) Busch, G. E.; Wilson, K. R. *J. Chem. Phys*. **1972**, *56*, 3655.

(38) Spence, M. A.; Levy, M. R. *J. Phys. Chem*., to be submitted for publication.